DYNAMICS OF CONTROLLED BOUNDARY LAYER SEPARATION ON A CIRCULAR CYLINDER

Václav Uruba, Milan Matějka, Pavel Procházka
Institute of Thermomechanics AS CR, v.v.i.

Summary

Dynamical aspects of the boundary layer separation on a circular cylinder in cross-flow are studied experimentally. Two cases are compared, the base case and the case with excitation using a synthetic jet actuator. The TR-PIV technique was used to catch both space and time velocity field correlations. Instantaneous velocity fields and skin friction distributions are evaluated. For dynamical structures study, the BOD method was applied based on energetic principle.

Dynamical modes connected with vortex shedding process, dynamical excitation by synthetic jet and transition to turbulence are identified.

Introduction

Cross flow over circular cylinder is one of the classical unsteady boundary layer separation canonical cases. It is a very good choice for demonstration of a boundary layer separation control strategies and mechanisms. The aim of the presented paper is to show physical mechanisms behind this phenomenon and influence of periodical excitation. We will concentrate on dynamical aspects of the phenomenon.

The classical approach to separation control involves steady suction in the separation region. However, this strategy proposed by Prandtl in his famous paper 1904 defining the notion of boundary layer, has practical disadvantages in using compressor and in low energetic efficiency. Nowadays, the commonly accepted control strategy for a bluff-body drag reduction involves excitation of the free shear layer periodically (see e.g. Greenblatt, Wygnanski, 2000). For this purpose the synthetic jet in the slot along the cylinder surface have been used.

In the case of wake behind a cylinder pseudo-periodical global behaviour could be observed forming well-known von Karman vortex street. However, periodically moving separated boundary layers form free shear layers subject to laminar-turbulent transition process.

Experimental setup

The model subjected to presented experiments was a cylinder in cross flow, diameter $D = 50$ mm, aspect ratio 5 and velocity of incoming flow around 6 m/s resulting in Reynolds number around 19 000. Thus, the wake was fully turbulent, however the boundary layer separation is of laminar nature as the Reynolds number is below critical value. After separation the free shear layer becomes turbulent very soon. The von Karman vortex street is born in the wake, the frequency is about 24 Hz

(corresponding to the Strouhal number 0.2). The situation is schematically depicted in Figure 1.
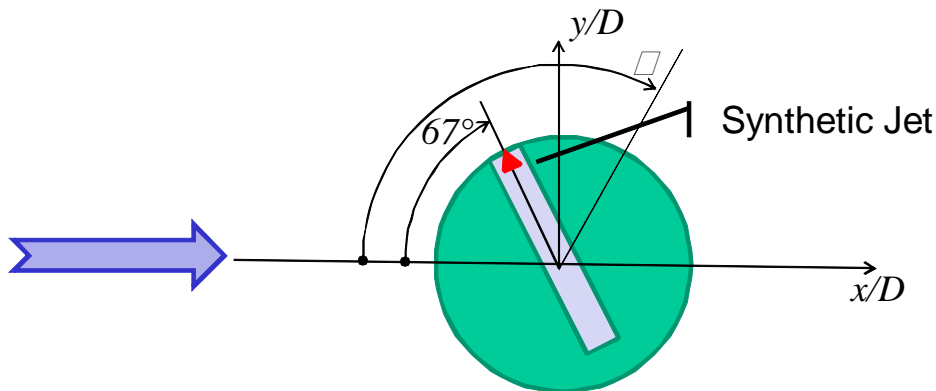

Fig.1 – Schematic view to the cylinder with actuator

Control strategy uses synthetic jet with slot along the cylinder surface. The slot of 1 mm in width was oriented along the cylinder axis in the angle 67° from the *x* direction. The actuator has been fabricated in the Czech Technical University in Prague using 10 loudspeakers 20 mm in diameter working in phase. The actuator is shown in Figure 2. The velocity in the slot orifice was sinusoidal in time with amplitude approx. 20 m/s and frequency 200 Hz.
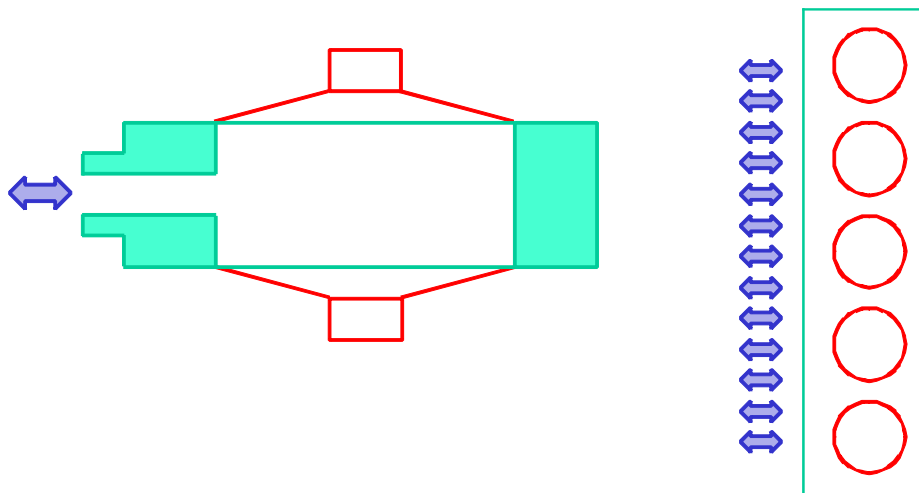

Fig.2 – Schematic view to the synthetic jet actuator

The time-resolved PIV method was used to resolve the instantaneous velocity fields. The measuring system DANTEC consists of laser with cylindrical optics and CMOS camera. Laser New Wave Pegasus Nd:YLF, double head, wavelength 527 nm, maximal frequency 10 kHz, a shot energy is 10 mJ for 1 kHz (corresponding power 2 x 10 W). Camera NanoSense MkIII, maximal resolution 1280 x 1024 pixels and corresponding maximal frequency 512 double-snaps per second. The camera internal memory 4 GB represents 1635 full resolution double-snaps. The maximal working frequency of the camera is limited by data rate, so it could be augmented by reducing its

resolution. In the experiments we used reduced resolution with maximal possible frequency, 1000 consecutive snaps were acquired and evaluated. As tracing particles the SAFEX smoke was applied. The software Dynamics Studio ver.2 was used for both data acquisition and velocity-fields evaluation by application of the adaptive correlation method.

Our sampling frequency 512 Hz in time domain was more then 2-times higher than the synthetic jet generator frequency (200. However, in actual configuration, we have no information about synthetic jet generation phase for a given individual snap. All measurements were carried out in the plane perpendicular to the cylinder axis located in the middle of the test section.

Instantaneous flow-field near the separation is monitored. Flow-field is analyzed using Proper Orthogonal Decomposition (POD) method and its generalization Bi-Orthogonal Decomposition (BOD).

The POD is considered to be a natural idea to replace the usual Fourier decomposition in nonhomogeneous directions. Adrian (2000) considers the POD as inhomogeneous filtering applied on the flow data in the framework of the LES method. The classical homogeneous filtering, using the Gaussian filter for example, is inconsistent with the fact that the turbulent eddies increase in size moving in traverse direction. This problem can be addressed by using the method of POD to construct low-pass filters that are inhomogeneous in one or more direction. The POD provides an optimal set of basis functions for an ensemble of data in the sense that it is the most efficient way of extracting the most energetic components of an infinite dimensional process with only a few modes.

The POD method is optimal in sense that the series of eigenmodes converges more rapidly (in quadratic mean) than any other representation. Convergence is very fast in the flows in which large coherent structures contain a major fraction of the total kinetic energy. As an example the pseudo-periodical vortex streets in wakes or strong shear layers could be mentioned.

The spatial quantities characterize the distributions in space, while temporal in time. According to the developers of the BOD themselves (Aubry, 1991) there is no real link between BOD and POD, since they are based on fundamentally different principles. In fact, BOD can be seen as a time-space symmetric version of the Karhunen-Loeve expansion or, in other words, a combination of the classical POD and the snapshot POD (see Tropea, 2007).

Results

Comparison of the base case without excitation (base case) with the case of excitation using synthetic jet (synthetic jet – SJ) are to be shown in details thereinafter.

The dynamical nature of the boundary separation phenomenon could be demonstrated using time evolution of skin friction along the cylinder surface. However, evaluation of the instantaneous local value on the skin friction experimentally is generally a complicated task. For this purpose we used the instantaneous velocity field measured by PIV technique. Then we interpolated the velocities on the line-arc located 0.7 mm above the cylinder surface. Then, the tangential component of the instantaneous velocity is considered as a measure of the skin friction in the given point and its instantaneous value could be estimated. Taking into account the fact that the interogation area size in approx. 0.4 mm, it is clear that the value of the skin friction

evaluated in this way is of the informative character only, however magnitude proportions and information on the instantaneous orientation is sufficiently evidential,
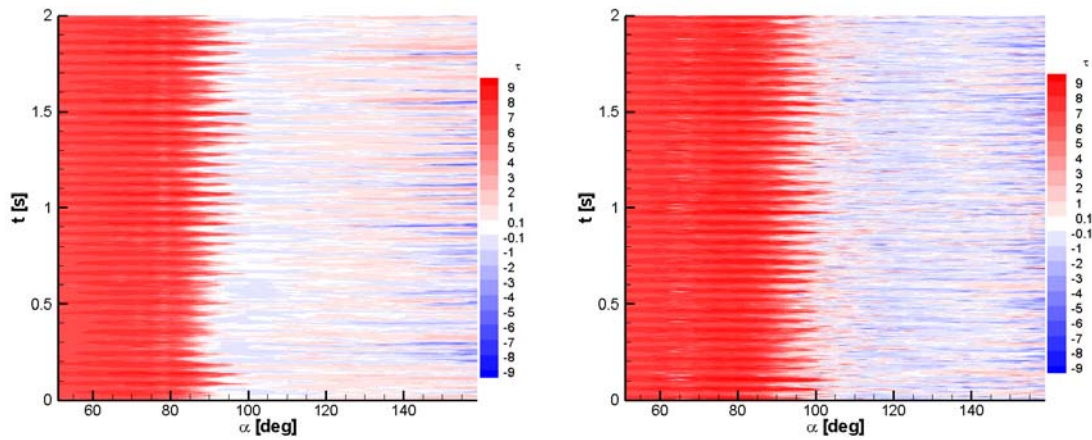

Fig.3 – Skin friction (base case – left, synthetic jet – right)

in our opinion.

In Figure 3 the time evolutions of the skin friction distribution along the cylinder surface is shown for both cases – without and with excitation. Red colour demonstrates positive skin friction orientation – the same as the main flow, while blue colour shows negative orientation – the back-flow. Situation with very small absolute value near the zero is characterized by white colour.

Attached flow (red colour) on the left part of the diagrams represents attached flow with distinct pseudo-periodical behaviour in time connected with vortex shedding phenomenon (frequency 24 Hz). The boundary position between positive and negative skin friction is for the controlled case (right graf) shifted downstream considerably. In the separation zone patterns of both positive and negative skin friction of very small absolute value could be seen indicating very complicated and dynamical system of separation bubles. Back-flow seems to be more intenseve in the controlled case. The results presented in Figure 3 are of qualitative nature.
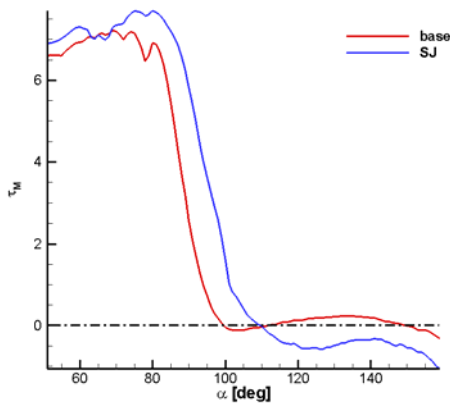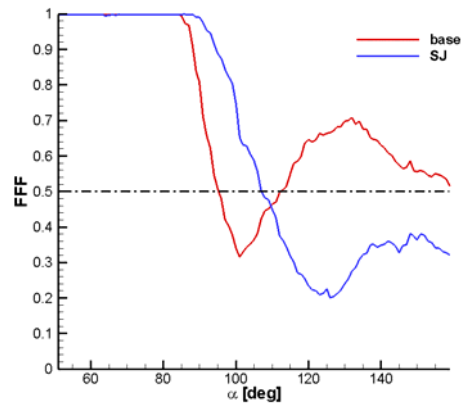

Fig.4 – Mean skin friction   Fig.5 – Flow forward fraction coefficient

Next, the time-mean pictures of the velocity fields are evaluated to determine position of the separation mean point. The classical definition of the mean point of separation could be based on mean value of the skin friction coefficient (Detachment) or on flow forward fraction (Transitory Detachment – see e.g. Simpson, 1996). The position of the Detachment is characterized by zero value of the mean skin friction and sign change from positive to negative for the first definition. Definition of the Transitory Detachment requires dropping the FFF coefficient value just below 0.5. (FFF stands for flow forward fraction coefficient). The calculated results of mean skin friction and FFF coefficient are shown in Figures 4 and 5. The evaluated positions α of Detachment is 98 deg for the base case and 108 deg for the control by synthetic jet, while Transitory Detachment is located 94 deg for the base case and 109 deg for the controlled case. Simpson claims that the position of Detachment and Transitory Detachment should be identical. Apparently it is not the case, however the differences are not very big.

Note: The values of evaluated position are much greater than in classical experiments because of 3D effects connected with low aspect ratio of our model.
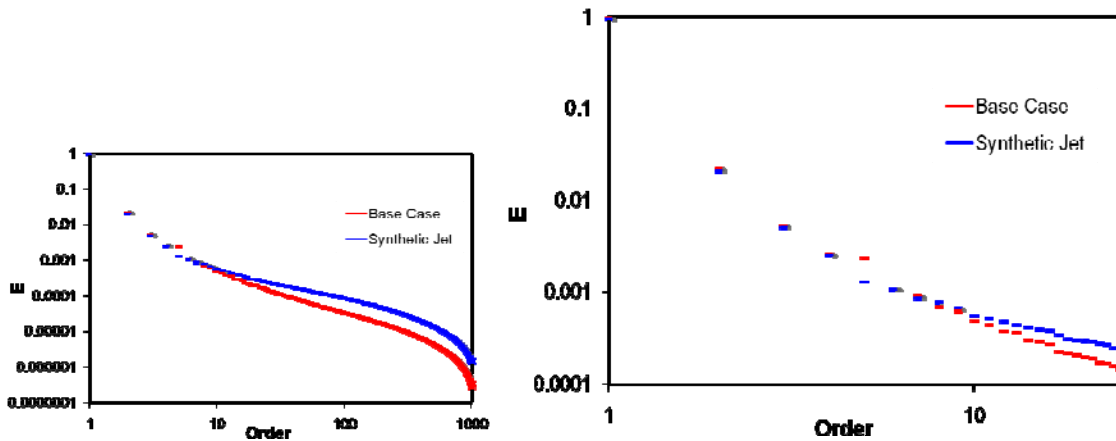

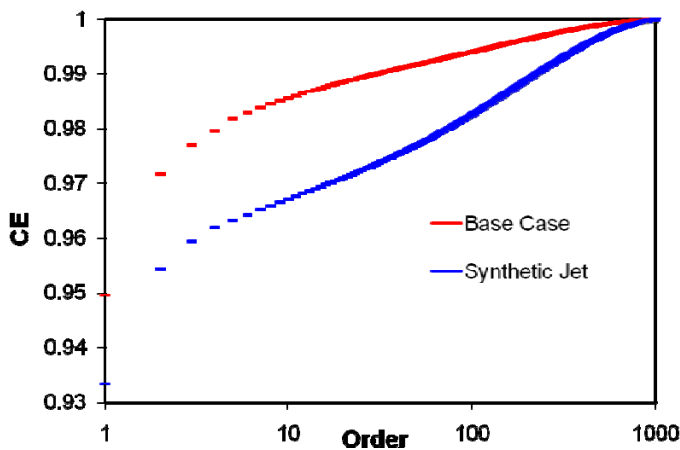Fig.6 – Modes relative energy (zoom – right)

Fig.7 – Cumulative energy of the modes

As a next step dynamical behaviour of the velocity field have been studied using BOD. The analyzed vector-fields result in 1000 energetical modes. The relative energy contents E in modes decreses rapidly with increasing order. Figure 6 shows this decay, energy of individual modes is related to the total kinetic energy of the velocity-field in question. (Both Energy and Order axes are logarithmical). Note that e.g. for the 10th mode

the corresponding energy represents less then 1 per mille of the total energy in both cases.
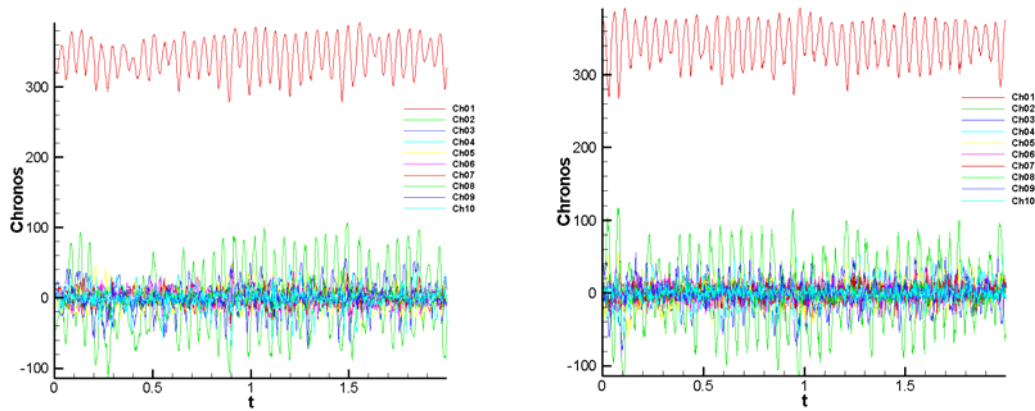

Fig.8 – Chronoses (base case – left, synthetic jet – right)

Then, figure 7 shows cumulative energy CE (again relative to the total energy, the cumulative energy axis is now linear) for all modes up to the indicated mode. Energy of the first 10 modes represents about 96 % of the total energy in the base case and about 98.5 % in the case of control using synthetic jet. Convergency of the energetical modes for the base case is more rapid then for the controlled case, however the diference is small in absolute values.

The time modes – Chronoses were analyzed in detailes. In Figure 8 there is comparison of the first 10 chronoses for the cases in question.

We see that an important value of the time-mean we obtained only for the first mode, higher modes are characterized by very small mean value. Quasiperiodical component is distingt for all modes, amlitude is decreasing with increasing mode order. From this it is clear, tht the first mode represents mainly mean picture of the flow-field and hihher modes are connected with velocity fluctuations, however in the first mode there is quasiperiodical component present as well.

It is clear that quasiperiodical nature of modes is connected with physical
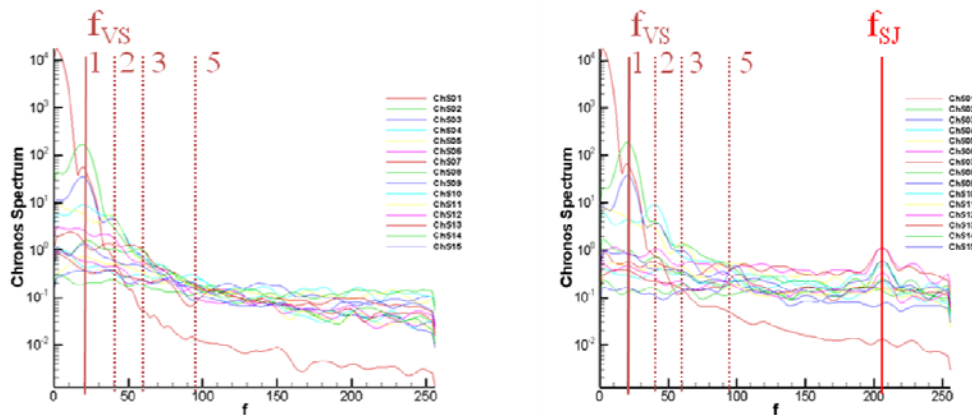

Fig.9 – Spectra of chronoses (base case – left, synthetic jet – right)

phenomena. In our case we could consider quasiperiodical vortex shedding (frequency 24 Hz) and periodical excitation using synthetic jet (frequency 200 Hz). To assign individual modes to physical phenomena we calculated spectra of the chronoses from Figure 8 – see Figure 9. The walch algorithm implemented in MATLAB software was used.

We could detect distinct peaks in spectra on various frequencies. Vortex shedding frequency f_{VS} with 1st, 2nd, 3rd and 5th harmonics and synthetic jet excitation frequency f_{SJ} are indicated in the figure. Now, qualitative analysis of spectra has been done with respect of presence of the frequencies. The results for the first 10 modes are shown in Table 1 for the base case and in Table 2 for the controlled case. The red color indicates "important" peak, yellow "light" peak and white corresponds to no activity on the given frequency.

Table 1 – Frequency peaks for modes, base case

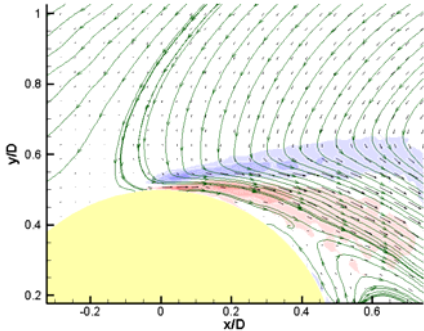| mode	f_{VS}	$2 f_{VS}$	$3 f_{VS}$	$5 f_{VS}$	f_{SJ}
1	●				
2	●				
3	●	●			
4	·	●		·	
5		●			
6	·				
7		·			
8	·	·			
9	·				
10					

Table 2 – Frequency peaks for modes, controlled case
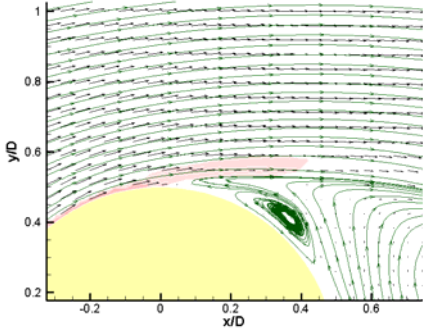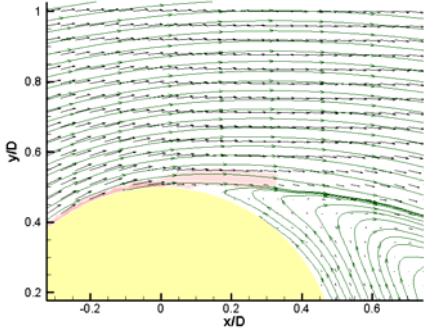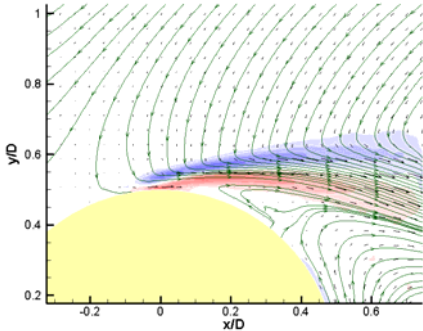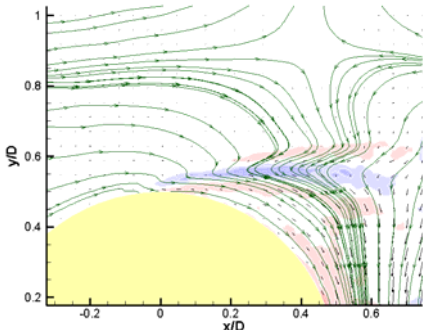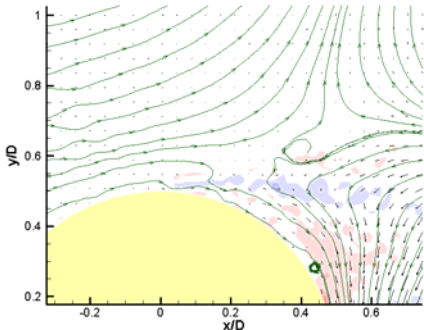
mode	f_{VS}	$2 f_{VS}$	$3 f_{VS}$	$5 f_{VS}$	f_{SJ}
1	●	·	·		
2	●	·	·		
3	●	·	·		
4		●			
5		·	●	·	
6		·			●
7					●
8		·		·	●
9					●
10		·	·	·	●

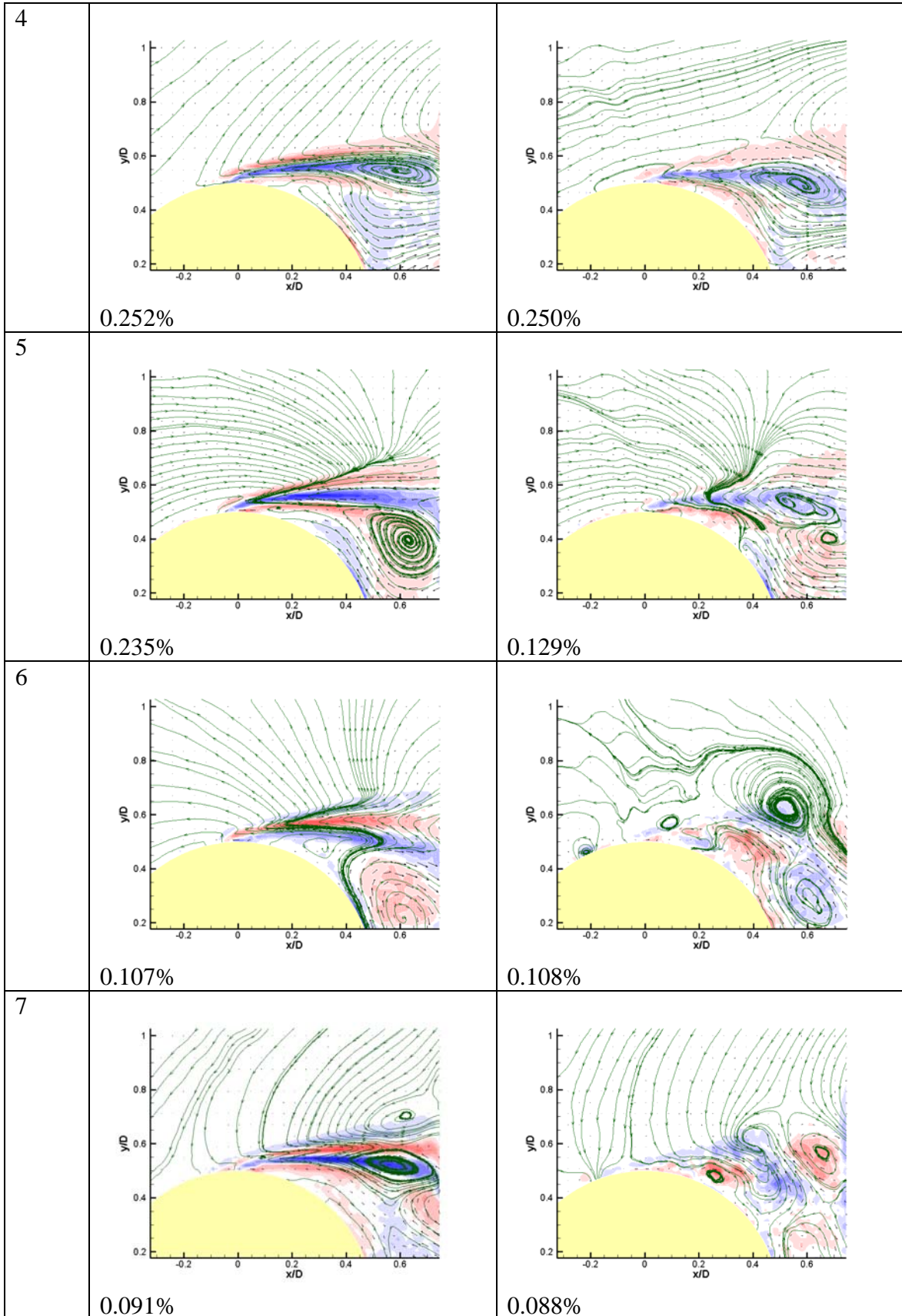The analysis shows clearly that the first 5 modes are connected with vortex shedding frequency and its higher harmonics. Higher modes exhibit very distinct peaks on the synthetic jet excitation frequency, however there are minor higher harmonic vortex shedding frequency peaks. Now, we are able to assign the individual modes to either vortex shedding or synthetic jet.
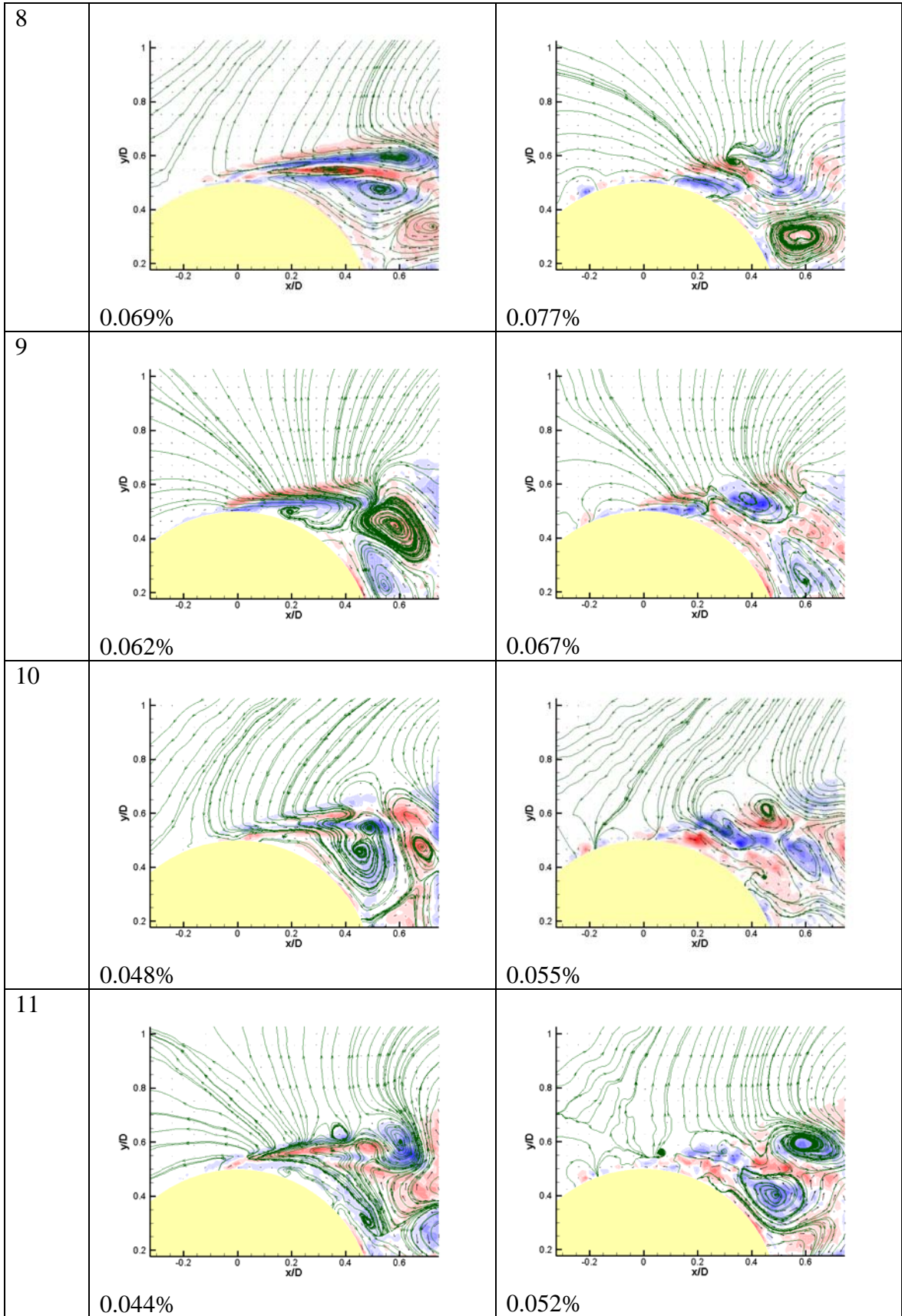
The first 15 topological modes – topoi are shown in the table in Figure 10. Base case is presented on the left, while controlled case is on the right. In the left lower

corner of each figure the energy content of the mode in question is given in percent of the total kinetic energy.

In all figures the flow is coming from left in *x* direction, the cylinder is depicted in yellow. The flow modes are visualized with help of streamlines added, red and blue colors represent positive and negative vorticity respectively generated by the mode.

mode	Base case	Synthetic Jet
1	95.00%	93.37%
2	2.18%	2.07%
3	0.53%	0.51%

4	0.252%	0.250%
5	0.235%	0.129%
6	0.107%	0.108%
7	0.091%	0.088%

8	 0.069%	 0.077%
9	 0.062%	 0.067%
10	 0.048%	 0.055%
11	 0.044%	 0.052%

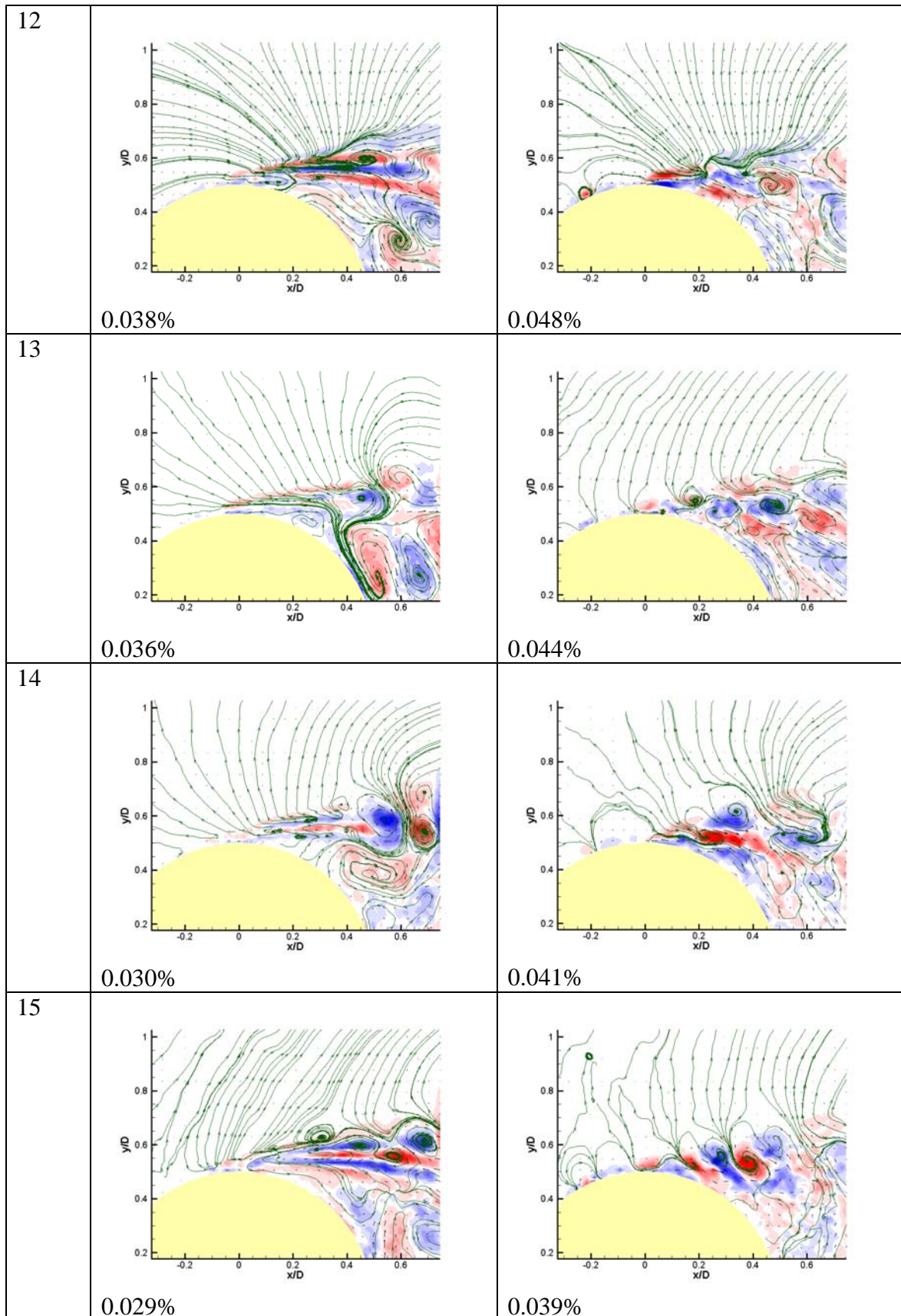|		
12	0.038%	0.048%
13	0.036%	0.044%
14	0.030%	0.041%
15	0.029%	0.039%

Fig.10 – Topoi (base case – left, synthetic jet – right)

In all figures the flow is coming from left in *x* direction, the cylinder is depicted in yellow. The modes are visualized with help of streamlines added, red and blue colors represent positive and negative vorticity respectively generated by the mode.

The fact that the modes 1-5 are similar for both cases suggests that physical mechanisms involved in the vortex shedding are very similar for both cases. The mode 1 represents itself the mean velocity field pattern, however frequency content on vortex shedding frequency is important for this mode in both cases as well. The mode 2 is characterized by the jet-like structures – one in the wake just below the mean shear layer, the second weaker is located in the cylinder leading part and with opposite orientation. This mode could be connected with entrainment process from outer region into boundary layer and free shear layer. Entrainment into the wake is characterized by the mode 3 forming a saddle point located above the wake. Modes 4 and 5 show big vortices within the free shear layer.

Modes 6 and higher differ considerably for the two cases. In the base case the higher modes could be characterized as more refined versions of the lower order modes. The controlled case is described by the system of small vortices within the shear layer. The modes of order higher than 10 are characterized by fine-grain structure of the free shear layer and wake. This picture suggests transition to turbulence of the free shear layer.

Conclusions

Behavior of the separated boundary layer forming free shear layer is different in the base case and the case of control by synthetic jet. While for the base case the free shear layer is subjected to gradual transition to turbulence through formation of more or less regular system of vortices, the controlled case is much more irregular, involving greater number of vortical structures small in size.

The perturbed region is much bigger for the controlled case despite of the fact that the mean picture shows narrower wake in this case.

References

Adrian R.J., Christensen K.T., and Liu Z.C. (2000) Analysis and interpretation of instantaneous turbulent velocity fields. Experiments in Fluids, Vol. 29, No. 3, pp.275-290.

Aubry N., Guyonnet R., Lima R. (1991) Spatiotemporal Analysis of Complex Signals: Theory and Applications, Journal of Statistical Physics, vol.64, Nos.2/3, pp.683-739.

Glezer, A., Amitay, M. (2002) Synthetic jets. Annu. Rev. Fluid Mech., 34, pp.503-529.

Greenblatt D., Wygnanski, I.J. (2000) The control of flow separation by periodic excitation. Progress in Aerospace Sciences, 36, pp.487-545.

Lumley J.L. (1967) The structure of inhomogeneous turbulent flows. Atm.Turb. and Radio Wave Prop., Yaglom and Tatarsky eds., Nauka, Moskva, pp.166-178.

Prandtl L.: Uber Flussigkeits bewegung bei sehr kleiner Reibung, Verhaldlg III Int. Math. Kong. (Heidelberg: Teubner), 1904, pp 484–491; Also available in translation as: Motion of fluids with very little viscosity. NACA TM 452 (March 1928).

Simpson, R.L., 1996, Aspects of turbulent boundary-layer separation, Prog.Aerospace Sci, vol.32, pp.457-521.

Tropea C., Yarin A.L., Foss J.F. eds. (2007) Springer Handbook of Experimental Fluid Mechanics.

Uruba, V. (2004) Receptivity of a free shear layer to excitation by a synthetic jet. (Eds.: Delville, J. - Bonnet, J. P. - Alvi, F.), Poitiers, Universite de Poitiers, 1st European Forum on Flow Control, Poitiers 04.10.11-04.10.14, pp.83-85.

Uruba, V. (2005) Flow control using synthetic jet actuators. Engineering Mechanics, vol. 12, No. 1, pp.41-62.

Uruba V., Knob M., Popelka L. (2006) Dynamics of a synthetic jet. Colloquium Fluid Dynamics 2006, Proceedings, Praha, Institute of Thermomechanics AS CR, (Eds.: Jonas, P., Uruba, V.), pp.137-140.

Uruba V., Knob M. (2007) Spatiotemporal Analysis of a Synthetic Jet Flow-Field. Conference Topical Problems of Fluid Mechanics 2007, Praha, IT AS CR, v.v.i., (Eds.: Prihoda J., Kozel K.), pp.185-188.

Uruba V. (2007) Boundary Layer Separation Dynamics. Conference Topical Problems of Fluid Mechanics 2008, Praha, IT AS CR, v.v.i., (Eds.: Prihoda J.; Kozel K.), pp.125-128.

Uruba, V.; Matejka, M., (2008) Dynamics of controlled boundary layer separation on a circular cylinder, EDRFCM 2008, 8-11 September 2008, Ostritz - St. Marienthal, pp.1-2.

Acknowledgement